



Journal of Advanced Research in Fluid Mechanics and Thermal Sciences

Journal homepage:
https://semarakilmu.com.my/journals/index.php/fluid_mechanics_thermal_sciences/index
ISSN: 2289-7879



Theoretical and Numerical Study on The Effect of Ambient Temperature Towards Gas Dispersion in Indoor Environment using CFD approach

Zaffry Hadi Mohd Juffry¹, Kamarulzaman Kamarudin^{1,*}, Abdul Hamid Adom¹, Muhammad Fahmi Miskon², Abdunasser Nabil Abdullah¹

¹ Faculty of Electrical Engineering Technology, Universiti Malaysia Perlis (UniMAP), 02600 Arau Perlis Malaysia

² Faculty of Electrical Engineering Universiti Teknikal Malaysia Melaka (UTeM), 76100 Durian Tunggal, Melaka Malaysia

ARTICLE INFO

ABSTRACT

Article history:

Received 5 December 2022

Received in revised form 26 March 2023

Accepted 5 April 2023

Available online 21 April 2023

Keywords:

Harmful gas dispersion; harmful gas behavior; thermofluids

The usage of harmful chemical gas and natural gas has been increasing rapidly which increase the risk of gas leakage incident to occur especially in the indoor environment. It is important to learn the gas dispersal behavior in order to mitigate the casualty caused by gas leakage. In addition, one of the factors that contribute to the dispersion of gas is temperature. This paper focuses to study the role of ambient temperature toward gas dispersion in an indoor environment by looking at the theoretical and numerical knowledge of gas diffusion's relationship with temperature. Computational Fluid Dynamics (CFD) has been utilized to simulate gas dispersion at different ambient temperature levels in an indoor environment. This study released ethanol vapor to simulate gas dispersion at 5°C, 25°C, and 40°C of ambient temperature to observe the way gas distribute in the indoor environment. Both results from the theoretical calculation and simulation were compared. The result indicates that the gas diffusivity has an increment of 3.5% for every 5°C increment of the temperature. This causes the gas to diffuse rapidly in the warm air compared to the cool air. This paper also finds out that when the initial ambient temperature which is 5°C, was increased to 25°C and 40°C it causes the spread distance of the gas increased by 13.75% and 32.50% respectively.

1. Introduction

Harmful chemical gaseous and hazardous contaminants airborne have been well-known nowadays. There are many types of different chemicals stored in the industrial building for processing the output product. Lack of awareness to keep and treat those chemical materials by the careful procedure will lead to the incident including explosions [1], fires, poisoning [2], extensive damage, and numerous casualties may be occurred. Recently, the incidence of gas leakage has increased gradually worldwide. One of the well-known gas leakage incidents happened on December 1984 which known as the Bhopal disaster. In this incident a pesticide plant that stored methyl isocyanate gas which more than 40 tons have been leakage and caused at least 3800 people's death [3]. In 2022,

* Corresponding author.

E-mail address: kamarulzaman@unimap.edu.my

<https://doi.org/10.37934/arfmts.105.1.194209>

there was an ammonia gas leakage from the industrial area which cause about 200 women workers in the contaminated area to fall sick because of inhalation from the ammonia gas. Most of the victims experience severe nausea, vomiting, and breathlessness after the inhalation of ammonia [4].

On other hand, gas dispersion in indoor environments also is a crucial concern, as it can pose significant risks to public health and safety. According to American Gas Association [5], approximately 187 million industrial, commercial, and residential buildings used natural gas every day. It is highly flammable, and gas leaks increase the risk of fire and explosion. Therefore, by looking at those major gas leakage incidents, it is important to study the behavior of the harmful gas leakage and the factors that cause the incident to happen. This is to plan the emergency evacuation and mitigate the risk of the gas leakage happening again in the future.

In order to mitigate these risks, it is important to understand the factors that contribute to gas dispersion and its spread in indoor environments. One of the key factors is ambient temperature. The relationship between temperature and gas dispersion is complex and not fully understood, but it is widely recognized that temperature can play a crucial role in determining the diffusion distance of harmful gases. To understand how the temperature is able to affect gas dispersion. Firstly, we have to understand the concept of the kinetic theory of gases. The kinetic theory of gases deals with the behavior of gas molecules and according to this theory, the molecules of all gasses are in continuous motion. For this reason, the kinetic energy has been transferred from one molecule to other molecules during the collision occurred. It led to the change of velocity for individual molecules [6]. The equation molar kinetic energy is as below:

$$E_m = \frac{3}{2}RT \quad (1)$$

From Eq. (1), the molar kinetic energy of the gas, E_m is proportional to its temperature, T , and the proportionality constant is $3/2$ times the gas constant, R . It demonstrates that a higher temperature will lead to a higher molar kinetic energy of the gas. There is also another gas law namely Charles Law that gives a details account of the relationship between the temperature and the volume of the gas. Its states that the volume of an ideal gas is directly proportional to the absolute temperature of the gas at constant pressure [7]. From the derivation of the equation obtained from Boyles's Law and Charles's Law then a new law namely as ideal gas law was generated. By looking at the Ideal gas Law, there is an obvious relationship between the pressure, volume, and temperature of the gas [8]. The ideal gas law is governed by Eq. (2) as below:

$$PV = nRT \quad (2)$$

where P is pressure, V is volume, n is the number of moles of gas, R is the ideal gas constant and T is temperature. The Ideal Gas Law assumes that gases are made up of large numbers of randomly moving particles that occupy a defined volume and that the total internal energy of a gas is directly proportional to its temperature. The law provides a useful approximation for many real gases under certain conditions, such as low pressure and high temperature.

Then, after knowing the basic concept of gas's relationship with the temperature, now we have to see more details on the relationship between the diffusion of gas and also temperature. Diffusion describes the movement of gas molecules from a higher concentration to a lower concentration region [9]. The relationship between the flow rate and the concentration difference is referred to as Fick's Law of Diffusion [10]. The diffusion coefficient is measured in square meters per second, m^2/s in SI units. Despite the slow nature of diffusion, even in gases, diffusion coefficients for gases at ordinary temperatures and one-atmosphere pressure primarily range from 10^{-5} to 10^{-4} m^2/s . In

contrast, diffusion coefficients for liquids and solutions are limited to the range of 10^{-10} to 10^{-9} m²/s. A rough estimate indicates that gases diffuse approximately 100,000 times more quickly than liquids. Diffusion coefficients increase with the increase in the absolute temperature. This means as the temperature increases the gas will rapidly spread into the air.

The utilization of Computational Fluid Dynamics (CFD) provides an opportunity to assess the potential harm of toxic gases as a risk indicator and offers the most precise prediction of gas dispersion compared to other mathematical models, such as Gaussian Plume and Lagrangian Particle Dispersion Models. Several studies have leveraged the exceptional accuracy of CFD modeling to evaluate toxic gas dispersion in industrial facilities. For example, Zhuang *et al.*, [11] utilized the CFD to study the gaseous contaminant's diffusivity in the indoor environment. Yang *et al.*, [12] used CFD simulations to analyze the impact of both flammability and toxicity in an offshore platform. The effectiveness of physical barriers [13], water curtains [14], and gas detector placement [15] can also be evaluated through three-dimensional CFD modeling of flammable and toxic gas dispersion. The results from CFD simulations can also be combined with dose-response models to determine the absorbed dose to the human body and to evaluate human fatality through methods such as Probit Analysis for the hydrogen fluoride gas leak in South Korea performed by Yang *et al.*, [16]. The result from the CFD simulation agreed with the collected data of actual dead vegetation. Argyropoulos *et al.*, [17] similarly utilized CFD results to assess the potentially toxic consequences of evacuation routes in the event of a toxic gas infiltrating the building. By running numerous time steps of CFD simulation from when someone starts to finish evacuating, these hazardous dose-response models can quantitatively analyze the toxic gas effects of planned evacuation routes. Syafiie *et al.*, [18] performed a CFD simulation to model the accidental indoor dispersion of chlorine from a small undetected leak in an indoor industrial space. The simulation focused on released chlorine gas to show various effects of temperature and wind velocity on the diffusion of heavy gas in a small indoor environment. However, this paper does not focus particularly on the effect of ambient temperature towards gas diffusion since in the simulation, they mentioned that the windows are open thus the wind velocities are assumed to be 1 m/s, 3 m/s and 5m/s which strong enough to affect the gas diffusion in indoor environment. It is not clear how the ambient temperature itself affect the gas distribution in indoor environment since most of the time the dispersion was affected by the strong wind flow. Furthermore, the paper does not perform the quantitative analysis in the result section. Only the qualitative result was presented which not giving clear picture the effect of ambient temperature towards gas dispersion itself.

In this study, we focus to investigate the effect of ambient temperature on gas dispersion inside the indoor environment. Current knowledge about the effect of temperature on the diffusion of gas will be calculated through theoretical and numerical methods. While CFD approach will be utilized to perform the simulation for the gas dispersion inside the indoor environment and the final result will be analyzed to observe the behavior of the gas concentration at different ambient temperatures. In this study also, we performed qualitative and quantitative methods to observe how significant the effect of ambient temperature toward gas dispersion in an indoor environment.

2. Methodology

This section presents the common mathematical equation involved in CFD computation, CFD environment modelling, and boundary setting to simulate the gas dispersion in the indoor environment at different ambient temperatures.

2.1 CFD Software and Governing Mathematical Equation

For this study, ANSYS/CFX 14.0 2020 has been selected to simulate the gas dispersion. This software is known to be a high-performance CFD software recognized for its robustness, high computation accuracy, and speed for gas analysis. In CFD, the basic equations that govern the conservation of mass, momentum, and energy balance are solved numerically for a given initial, flow domain, and boundary conditions. It is necessary to briefly review those governing equations that are relevant to the issue of gas dispersion in different ambient temperatures.

The Continuity Equation:

$$\frac{\partial \rho}{\partial t} + \frac{\partial(\rho u_i)}{\partial x_i} = 0 \quad (3)$$

Momentum balance:

$$\frac{\partial \rho u_i}{\partial t} + \frac{\partial(\rho u_i u_j)}{\partial x_j} = -\frac{\partial p}{\partial x_i} + \frac{\partial}{\partial x_j} \left[\mu \left(\frac{\partial u_i}{\partial x_j} + \frac{\partial u_j}{\partial x_i} \right) + \lambda \frac{\partial u_k}{\partial x_k} \right] + \rho g_i \quad (4)$$

here, ρ is the density, u_i is the velocity component in the i^{th} direction, p is the pressure, μ is the viscosity of the medium, λ is the second coefficient viscosity (the term involving this variable is assumed to be negligible) and g_i is the component of gravitational acceleration in the i^{th} direction.

For buoyancy computation, a source term is added to the momentum equations as follows:

$$S_{M,buoy} = (\rho - \rho_{ref})g \quad (5)$$

which can be approximated by Boussinesq Model:

$$\rho - \rho_{ref} = -\rho_{ref}\beta(T - T_{ref}) \quad (6)$$

where β is the thermal expansivity and T_{ref} is the buoyancy reference temperature:

$$\beta = -\frac{1}{\rho} \frac{\partial \rho}{\partial T} \Big|_p \quad (7)$$

Diffusive Transport Equation:

The general form of the diffusive transport equation for the additional variable scalar is:

$$\frac{\partial(\rho\phi)}{\partial t} = \nabla \cdot (\rho D_\phi \nabla \phi) + S_\phi \quad (8)$$

where ρ is the mixture density, ϕ is the gas quantity per unit volume or concentration, ϕ is gas mass concentration, S_ϕ is a volumetric source term of the gas and D_ϕ is the kinematic diffusivity of the gas through the air.

For turbulent flow, this equation is Reynolds-averaged and becomes:

$$\frac{\partial(\rho\phi)}{\partial t} = \nabla \cdot \left((\rho D_\phi + \frac{\mu_t}{Sc_t}) \nabla \cdot \phi \right) + S_\phi \quad (9)$$

where μ_t is the turbulence viscosity, and S_{C_t} is the turbulence Schmidt number, which takes a constant value of 0.9 for thermal buoyancy-driven flows modeled using the Boussinesq approach. For details see [19].

2.2 CFD Modelling and Configuration

The experiment simulated the dispersion of harmful gas inside a closed empty testbed platform geometry shape illustrated in Figure 1. The design of the model is the same as the integrated mobile gas sensing testbed [20] located in the Centre of Excellence for Advance Sensor Technology (CEASTech), Universiti Malaysia Perlis. The testbed was developed to capture the reading of gas dispersion on the platform. However, the environment in which the platform was placed cannot be controlled, especially ambient temperature and the resolution of the testbed is relatively low since the platform was only installed with 72 numbers of gas sensors. Therefore, this study chose to develop a CFD model of the platform that is able to control different environmental parameters. The CFD model has 6m (length) x 3m (width) x 0.5 (height). It consists of four adiabatic non-slip walls, an adiabatic ceiling, and an adiabatic flat floor. There will be no presence of obstacles inside the platform except for the side of the walls. This is to prevent the obstacle influence the dispersion of the gas. The dispersion of gas inside the platform must significantly affect by the ambient temperature itself. A petri dish that contained ethanol solution was placed at the location of (x = 1.5m, y = 3m) which is known to be the center of the CFD model to simulate the release point of the harmful gas. Ethanol vapor will be used in this research to simulate the harmful gas release since it is widely used in mobile robot olfaction experiments to simulate harmful gas leakage [1,21-23]. All the details on the boundary conditions are shown in Table 1.

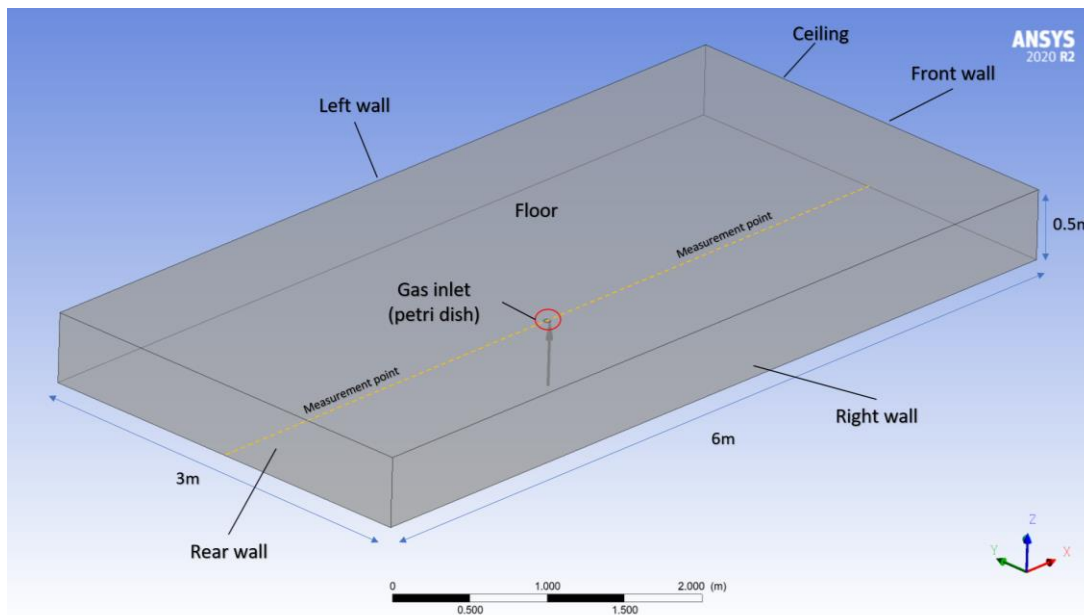


Fig. 1. Three-Dimensional (3D) geometry closed testbed model

Table 1

Boundary condition of the CFD model

Boundary	Type	Details
Petri dish (Diameter: 0.06m)	inlet	Gas Type: CH_3CH_2OH (ethanol vapor) Mass flow rate: 0.01kg/s
All walls, ceilings, and floor	wall	adiabatic

The tetrahedron mesh type was applied in this model to fill up the model space. The mesh has an element size of 0.2m^2 and produced about 108,187 total numbers of elements and 21,253 total number of nodes as shown in Figure 2. The previous researcher which is Zhuang *et al.*, [11] performed an experiment with three different mesh sizes and he finds out that the final CFD computation result does not depend on the mesh size. Therefore, the number of mesh produces in this model is sufficient to run the simulation and also helps to reduce computer computation time. Hence, this study will not run any experiment related to the comparison between different mesh numbers for the number of mesh validation.

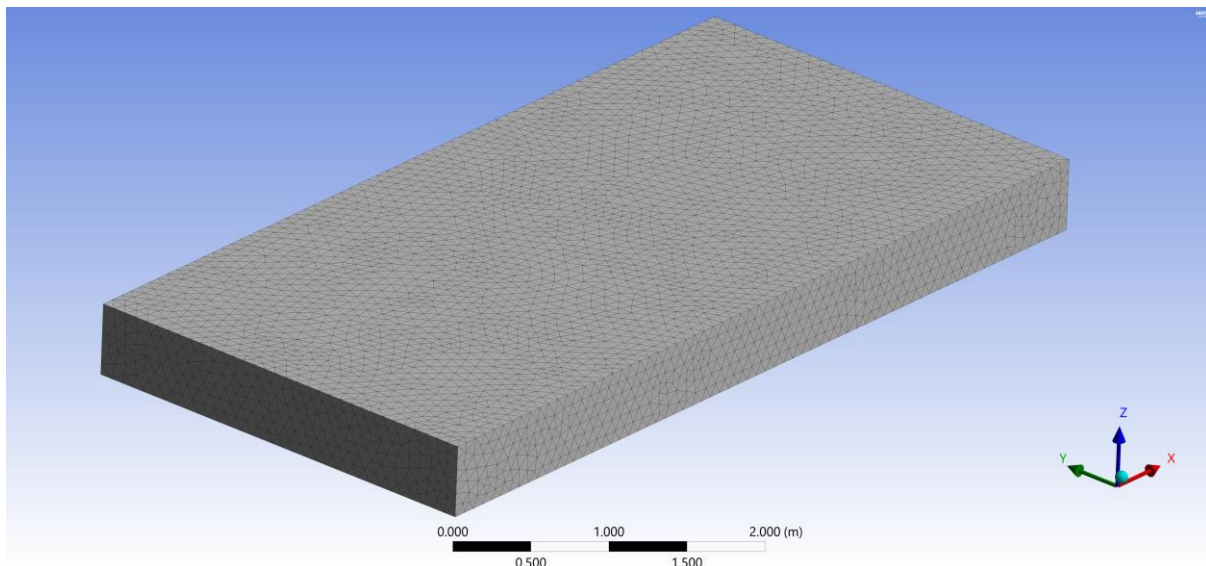


Fig. 2. Mesh grid for the testbed model

The simulations of the harmful gas dispersion performed on Intel® i5 Core computer. The gas was emitted through the simulated petri dish which has been treated as an inlet boundary condition type with a constant emission rate as stated in Table 1. The difference in this experimental setup was only the initial condition of the ambient temperature. The initial ambient temperature was set up to three different level which is 5°C (i.e., cold condition), 25°C (i.e., normal condition), and 40°C (i.e., warm condition), while the relative humidity will be maintained at 50%.

The experiment setup has been run for both transient and steady-state analysis. For transient analysis, the total simulation time for each simulation is 60 seconds with a step size of 0.25 seconds. Initial spreading calculations with a time step of 0.10 seconds were performed and the comparison showed that a step size of 0.25 seconds would be adequate. Therefore, there are 240 total steps generated from the CFD simulation result. In addition, to ensure the gas dispersion is only affected by ambient temperature and not by other parameters (e.g., wind) there is no significant airflow introduced in the CFD models and the air turbulence also will be relatively low. Since the air velocities in the present study are fairly low and no heat transfer is considered, it is expected that no special, wall-induced effect will be encountered.

Upon conducting both transient and steady-state CFD simulations, the concentration profiles of the dispersed ethanol vapor were analyzed and compared. The results from the CFD simulations enabled the revelation of the significance of ambient temperature in indoor environments to the process of gas dispersion.

3. Results

3.1 Theoretical Study on The Role of Ambient Temperature on The Diffusion of Gas in The Indoor Environment

The harmful gas contaminants are basically one type of molecule same as the molecule of the air and naturally, they can diffuse into the air. Diffusion describes the movement of gas molecules from a higher concentration to a lower concentration region. The diffusion process of the gas molecules into the air is governed by Fick's first law and Fick's second law:

$$J = -D\nabla C \quad (10)$$

$$\frac{\partial C}{\partial t} = \nabla \cdot (D \nabla C) \quad (11)$$

From Eq. (10) and Eq. (11), J is the "diffusion flux" (i.e., the amount of the gaseous contaminant per unit area per unit time), D is the diffusion coefficient or known to be diffusivity of the gas in the air while C is the volumetric concentration of the gas contaminants.

The diffusion coefficient or diffusivity of the gas with the air can be obtained from the equation derived by Cussler *et al.*, [24].

$$D = \frac{1.858 \times 10^{-3} T^{\frac{3}{2}}}{p \sigma_{AB}^2 \Omega} \sqrt{\frac{1}{M_A} + \frac{1}{M_B}} \quad (12)$$

From Eq. (12), A and B are kindly indicating two different gaseous to be diffused into each other. T is the absolute temperature in degrees Kelvin, p is the pressure, M is the molar mass of each type of gas, $\sigma_{AB} = (\sigma^A + \sigma^B)/2$ which is the average collision diameter between the molecule, and Ω is the temperature-dependent collision integral. This equation shows that the diffusivity is positively associated with the absolute temperatures of the gas and air. According to the kinetic theory of the gases, all diffusivities increase with the temperature and pressure. For example, Figure 3 shows the change of the ethanol diffusivity with the change in the absolute temperature of the ethanol and air. Based on the graph, the ethanol diffusivity is directly proportional to the absolute temperature. As the absolute temperature increases the diffusion coefficient between ethanol and air also increases. The diffusion coefficient of Ethanol and air has an increment of 3.5% for every 5°C increment of the absolute temperature. It means that as the diffusion coefficient of ethanol increases, it will rapidly diffuse into the air. At 5°C, the ethanol has a reading of diffusion coefficient with 0.104 cm^2/s while at 40 °C, it has the reading with 0.130 cm^2/s which has an increment of 25%.

For further observation, a simplified one-dimension model is shown in Figure 4. A long pipe model with 3m in the length is lying horizontally. Since the distance from the contaminant source to the ventilation exhaust in most indoor environments are in the range of 3m, so this length of magnitude was chosen. The ethanol vapor will be released at different absolute temperatures to let it diffuse into the pipe from the left (i.e., Point A) to the right end of the pipe (i.e., Point B) which is maintained at zero concentration. Then the difference in the ethanol concentration in the pipe is observed.

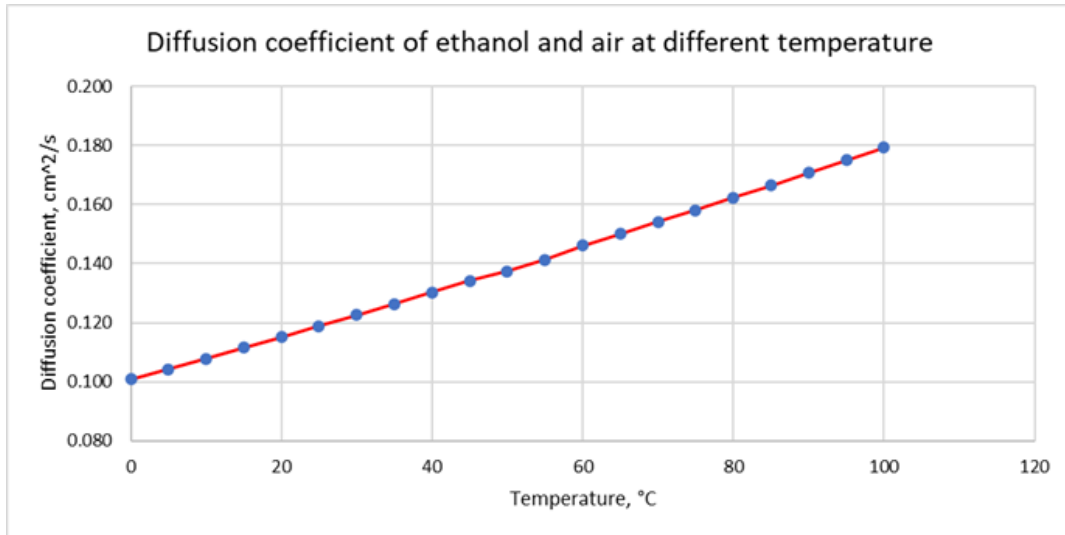


Fig. 3. Rate of ethanol diffusivity into the air at different temperatures

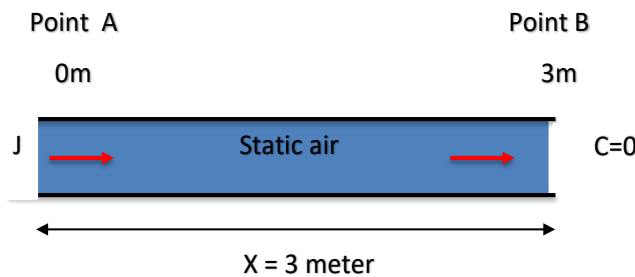


Fig. 4. Diffusion of ethanol in the static air

From the above model, it is assumed that the air inside the pipe is static. This is to ensure that the diffusion of the ethanol is only affected by the difference in absolute temperature of both gases. In this study, three different temperature reading at 5°C, 25°C, and 40°C were chosen. Therefore, the diffusivity values of the ethanol will be different from each other depending on the temperature level. For one-dimension (1D) situations such model above, Eq. (10) and equation Eq. (11) can be simplified as below:

$$J = -D \nabla \frac{\partial C}{\partial x} \tag{13}$$

$$\frac{\partial C}{\partial t} = D \frac{\partial^2 C}{\partial x^2} \tag{14}$$

when a steady-state is achieved, there is no diffusion occurs. Therefore, $\frac{\partial C}{\partial t} = 0$, and Eq. (13) can be simplified as

$$\frac{\partial^2 C}{\partial x^2} = 0 \tag{15}$$

with boundary conditions of $\frac{\partial C}{\partial x} = -\frac{J}{D}$ for $X = 0$, while $C = 0$ for $X = 3$, therefore has the following equation under the steady-state condition:

$$C = \frac{J}{D} (3 - x) \tag{16}$$

when Eq. (16) is applied for ethanol diffusion in the horizontal pipe model at a different temperature, the concentration profile of ethanol at different temperature level are shown in Figure 5. Based on the plot graph of the concentration of ethanol and length of the pipe above, the concentration of the gas inside the pipe is diverse at different levels of temperature. It shows that the concentration of ethanol tends to be zero concentration at a faster rate when the temperature is high. The difference between the concentration of ethanol at 5°C and 40°C is 25% while the difference between the concentration of ethanol at 5°C and 25°C is 14%. The reason is that when the temperature tends to be increased, it will also increase the diffusivity of the ethanol gas into the air inside the pipe. Therefore, any gases will diffuse rapidly when the temperature is high.

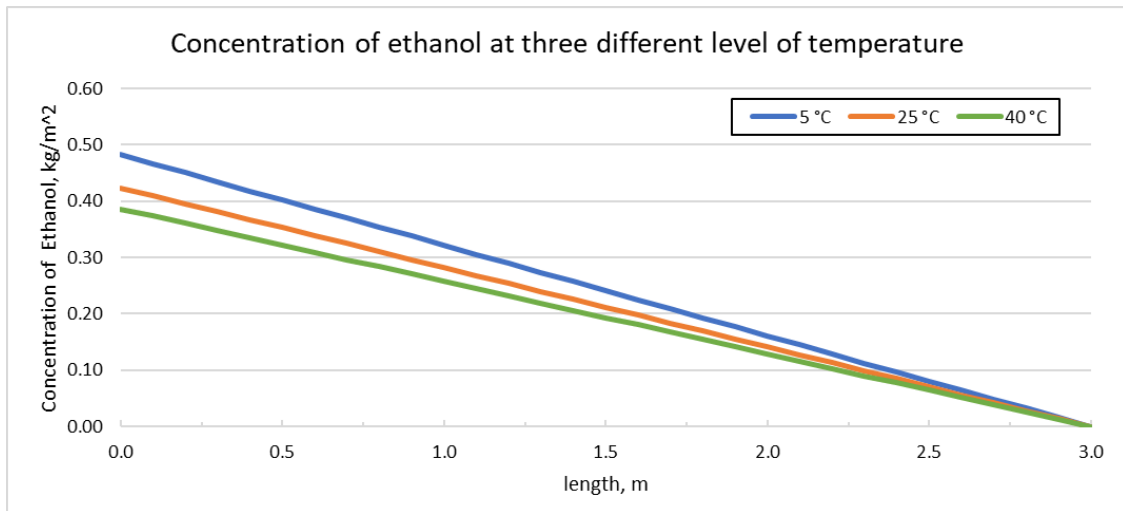


Fig. 5. Ethanol concentration profile inside the pipe at different temperatures

Now, this study will observe the effect of temperature with the distance of ethanol needed to diffuse from Point A at constant concentration until it reaches zero concentration at Point B. Here, from equation 4.5 we simplify the equation as below:

$$L = C \frac{D}{J} \tag{17}$$

from Eq. (16), the concentration of Ethanol, C , and the diffusion flux, J will be held constant. The difference will be in the diffusivity value of the ethanol, D at different temperatures. Through the calculation of Eq. (17), it was determined that at a temperature of 5°C, a length of 3m of pipe was required for the ethanol concentration to reach zero. However, when the temperature was increased to 25°C, the required length increased to 3.4m, representing a 13% increase in the length of the pipe. At 40°C, a length of 3.7m was necessary, resulting in a 23% increase. These results demonstrate that when the gas is released at a warm temperature, it will increase the spread distance of the gas. While, when the gas is released at a cold temperature it will decrease the spread of the gas distance. This phenomenon is attributed to the increase in kinetic molecular energy of the gas at higher temperatures, causing frequent collisions between the molecules and leading to their diffusion over a greater distance.

3.2 Comparison of Concentration Contour from CFD Simulation

This section will discuss the results gained from the ethanol dispersion simulation at different ambient temperatures (i.e., 5°C, 25°C, and 40°C). The concentration contour of three simulation results has been obtained on the transverse plane at $z = 0.01\text{m}$ for comparison. The ethanol was released at the center of the simulated testbed platform for 1 minute and the simulation transient result for every 10 seconds of the gas spread is shown in Figure 6. From the figure, it can be observed clearly that there are some differences between the concentration contour of ethanol at different levels of ambient temperature. The spread of the ethanol is not similar even though the mass flow rate of the source for all the simulation are similar. At the early stage of the dispersion, the ethanol tends to spread in a circular manner. Then, it spread until it reaches the testbed's side wall and continues to spread to another region. In 30 seconds and above, all the testbed area has been completely covered by the ethanol concentration. These comparisons result implied that at high ambient temperature, the gas tends to spread (i.e., diffuse) faster compared to low ambient temperature.

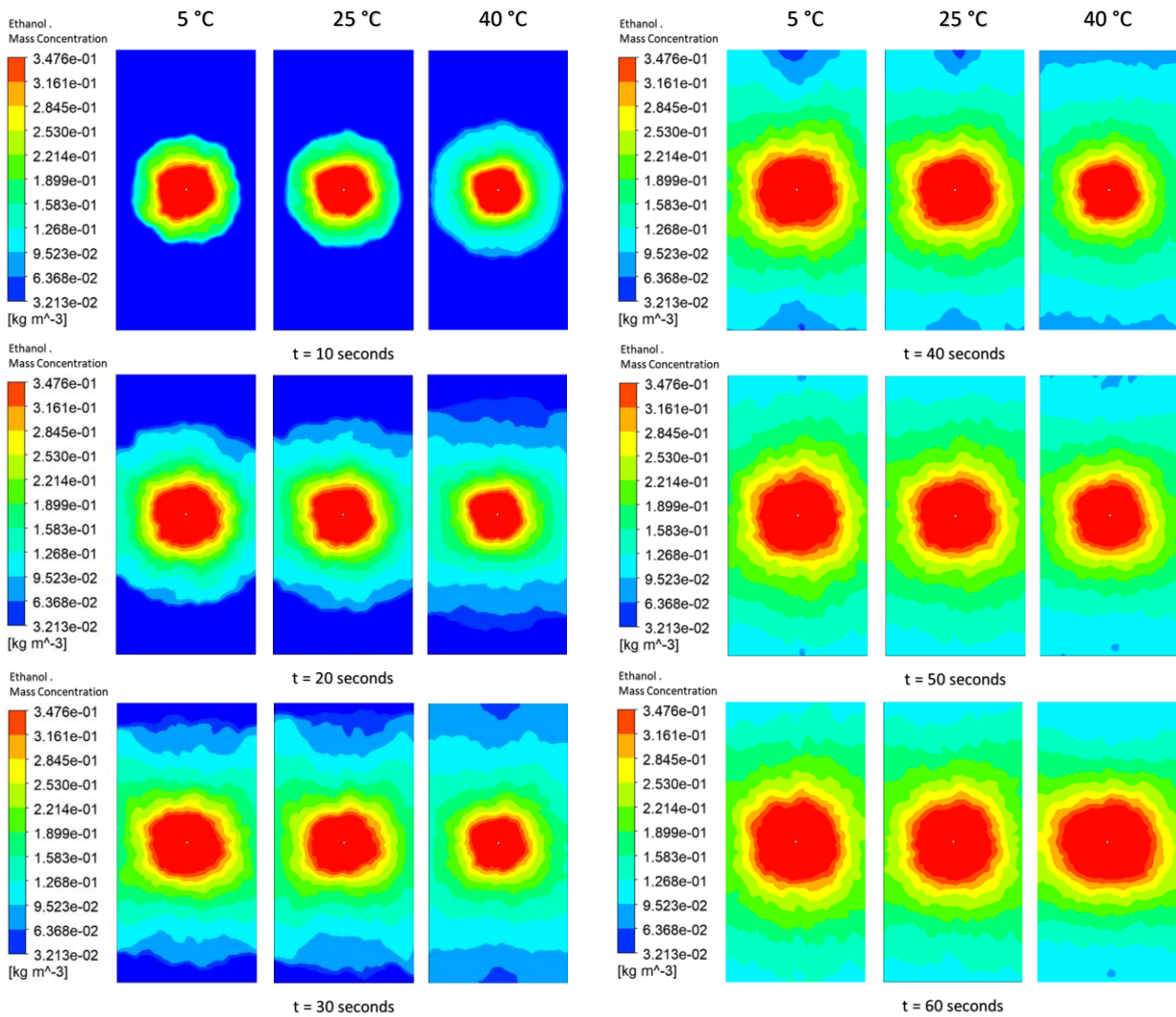


Fig. 6. Ethanol concentration contour at different ambient temperatures and time

Figure 7 compares their ethanol concentration at steady-state conditions. By taking very careful visual inspection, the concentration of the ethanol spreads is completely different in terms of concentration contour and also the spreading area. As the ethanol is dispersed away from the source, the gas will mix with air and resulting in the decrease of ethanol concentration along with the distance. In addition, as the ambient temperature increases the distance of the ethanol dispersion also increased. This result is consistent with the theoretical findings in section 3.1 of this paper.

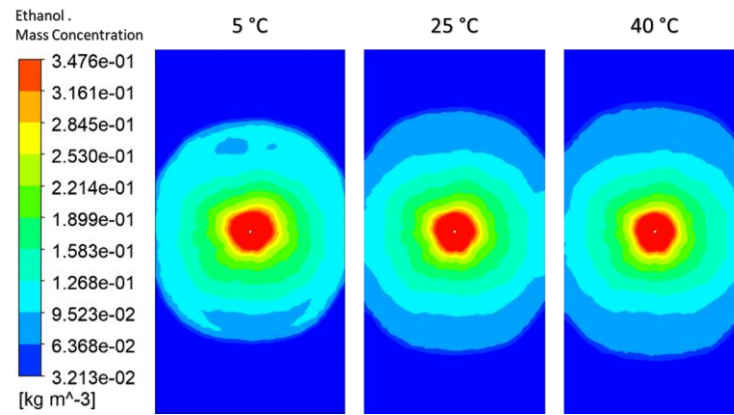


Fig. 7. Ethanol concentration profile at steady-state condition

3.3 Percentage Deviation Contours

In this section, an index known as the percentage deviation (PD) is introduced as a means to quantitatively evaluate the difference in ethanol concentration profile. This is necessary as visual inspection alone is not considered to be a sufficient method, due to its lack of accuracy and rigor. The following equation has been utilized to obtain quantitative results:

$$PD = \frac{|C_A - C_B|}{C_B} \times 100\% \quad (18)$$

where PD is the percentage deviation, C_A and C_B is the concentration reading at a particular point on the horizontal z-plane (i.e., 0.01m) for two different result samples. This study will observe the significant difference between the concentration of ethanol at different ambient temperatures. If the PD values were greater than 5% in 50% of the sample plane, then the difference between the concentration will be considered as significant.

From contour maps in Figure 6, when $t=10$ seconds, the concentration difference (i.e., $PD > 5\%$) between 5°C and 25°C is 84.91% of the sample plane area. While the difference (i.e., $PD > 5\%$) between 5°C and 40°C is 96.54% of the sample plane area. Both of the concentration differences (i.e., $PD > 5\%$) are more than 50%. After 30 seconds of dispersion (i.e., $t = 30$ seconds), the concentration difference between 5°C and 25°C started to reduce to about 66.33% while the concentration difference between 5°C and 40°C was reduced to 80.33% from the sample point. Then, after the time of dispersion falls between $t= 40$ seconds to $t= 60$ seconds, most of the outstanding area (i.e., an area where $PD > 5\%$) for concentration difference between 5°C and 25°C and concentration difference between 5°C and 40°C reduces to about 40.50% and 72% respectively.

In a steady-state condition, as depicted in the contour maps in Figure 7, it was determined that there was a 65.90% concentration difference (i.e., $PD > 5\%$) across the sample plane area for an ambient temperature level between 5°C and 25°C . Furthermore, when the ambient temperature level was increased to 40°C , the concentration difference (i.e., $PD > 5\%$) across the sample plane area

increased to 70%. These observations, both in steady-state and transient results, suggest that higher ambient temperature results in a greater difference in the concentration of ethanol compared to lower temperatures. Table 2 and Table 3 show the summary of PD values of ethanol concentration for transient and steady-state results respectively.

Table 2

Percentage Deviation (i.e., PD > 5%) values of the transient results

Ambient Temp. Comparison	10 sec	20 sec	30sec	40sec	50sec	60sec
5°C and 25°C	84.91%	75.64%	66.33%	64.17%	59.33%	40.50%
5°C and 40°C	96.54%	90.89%	80.33%	80.17%	79.17%	72.00%

Table 3

Percentage Deviation (i.e., PD > 5%) values of the steady-state results

Ambient Temp. Comparison	Steady-state
5°C and 25°C	65.90%
5°C and 40°C	70.00%

3.4 Dispersion Distance Comparison

The present section endeavors to compare the dispersion distance of ethanol concentration in the simulation outcome. The information on the ethanol concentration at a particular point was recorded and contrasted at varying ambient temperatures, as shown in Figure 8. The measurements of 600 samples of ethanol mass concentration were taken along the yellow line shown in Figure 1. It shows the ethanol concentration profile for each ethanol dispersion distance at different ambient temperature levels (i.e., 5°C, 25°C, and 40°C) at transient and steady-state conditions.

As depicted in Figure 8, the ethanol concentration profile at $t = 10$ seconds demonstrates a significant variation in terms of dispersion distance when the gas is released at different ambient temperatures. The dispersion of the gas tends to travel a greater distance when it is released in warm air, as opposed to cooler temperatures. Note that, all parameters of the simulation were held constant, with the exception of ambient temperature. Further insight into the variations can be observed by examining Figure 9, which illustrates the Region of Interest (ROI) of ethanol concentration at the point of maximum dispersion. At 5°C, when $t = 10$ seconds the gas dispersed at a distance of 2.40m. However, when the temperature increased to 25°C and 40°C the distance of dispersion has an increment of 13.75% and 32.50% respectively. Specifically, it is observed that variations in ambient temperature significantly impact the dispersion distance of the gas.

From Figure 10, it can be observed that there was also a difference in the dispersion length of the ethanol at different ambient temperatures during the steady-state condition. To get a better visualization of the difference, Figure 11 plots the ROI of ethanol concentration which on the tip of the dispersion. Now, the difference can be seen clearly, at 5°C the ethanol molecule tends to diffuse shorter distances compared to when the ambient temperature at 25°C and 40°C. By the quantitative, the distance of the ethanol diffusion increases by 10.36% when the ambient temperature increases from 5°C to 25°C. While the dispersion distance has the increment up to 15.03% when the ambient temperature further increases to 40°C. This result agrees with the theoretical calculation in section 3.1.

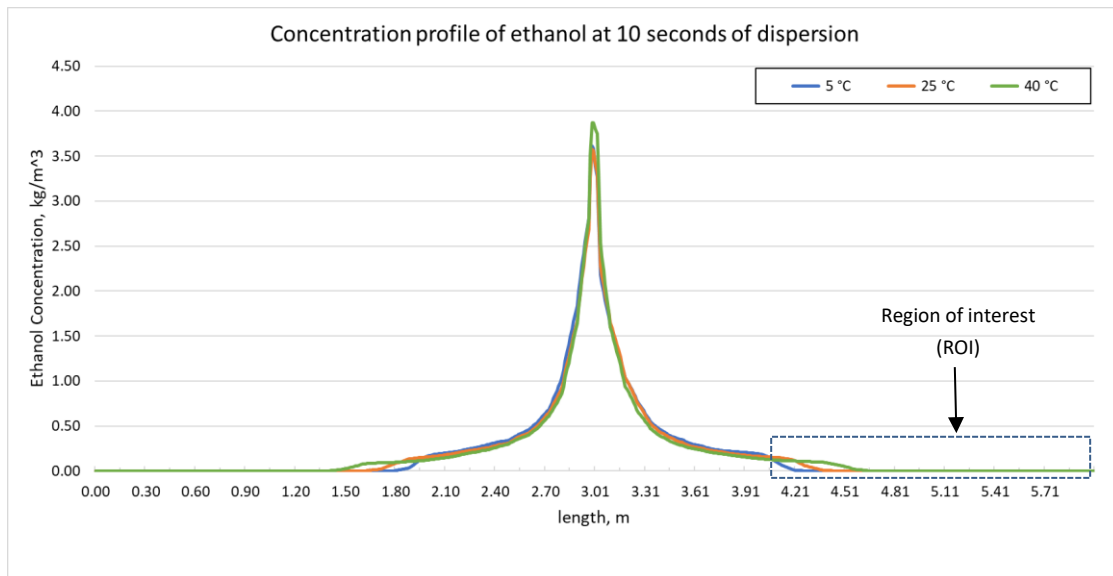


Fig. 8. Ethanol concentration profile released at different ambient temperatures (transient $t=10$ seconds)

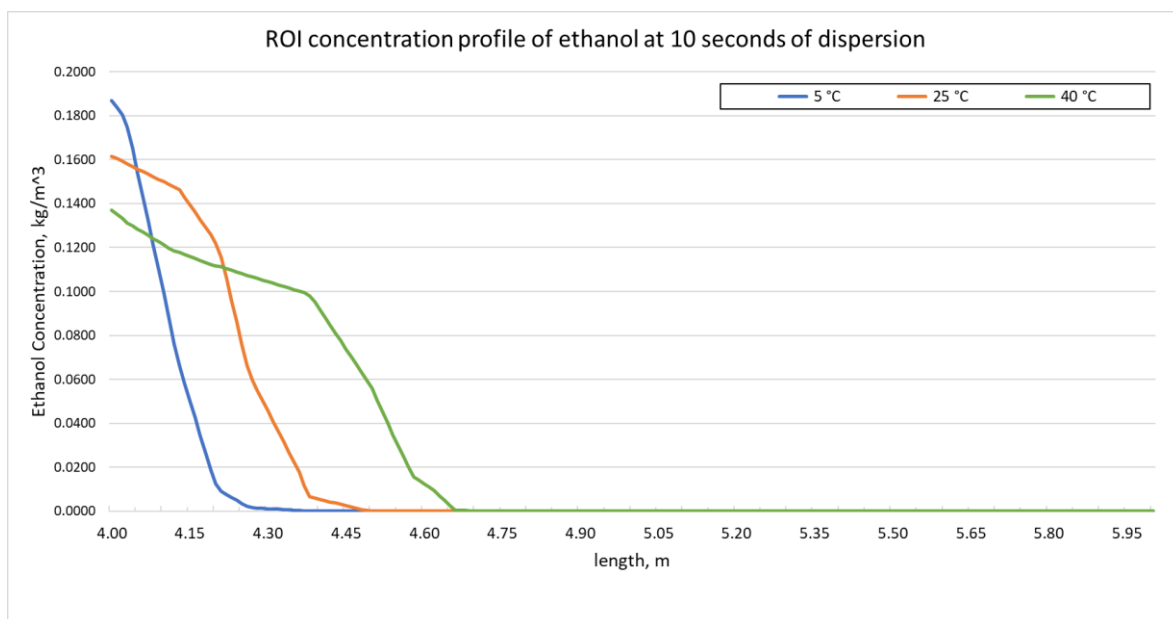


Fig. 9. Ethanol concentration profile at the tip region of the dispersion (transient $t = 10$ seconds)

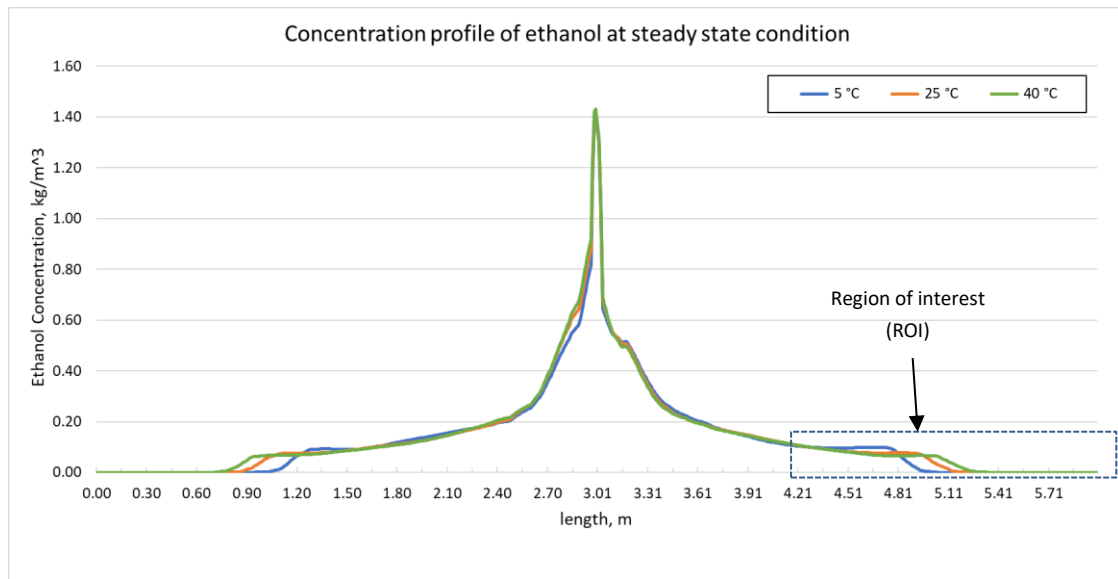


Fig. 10. Ethanol concentration profile released at different ambient temperature (steady-state)

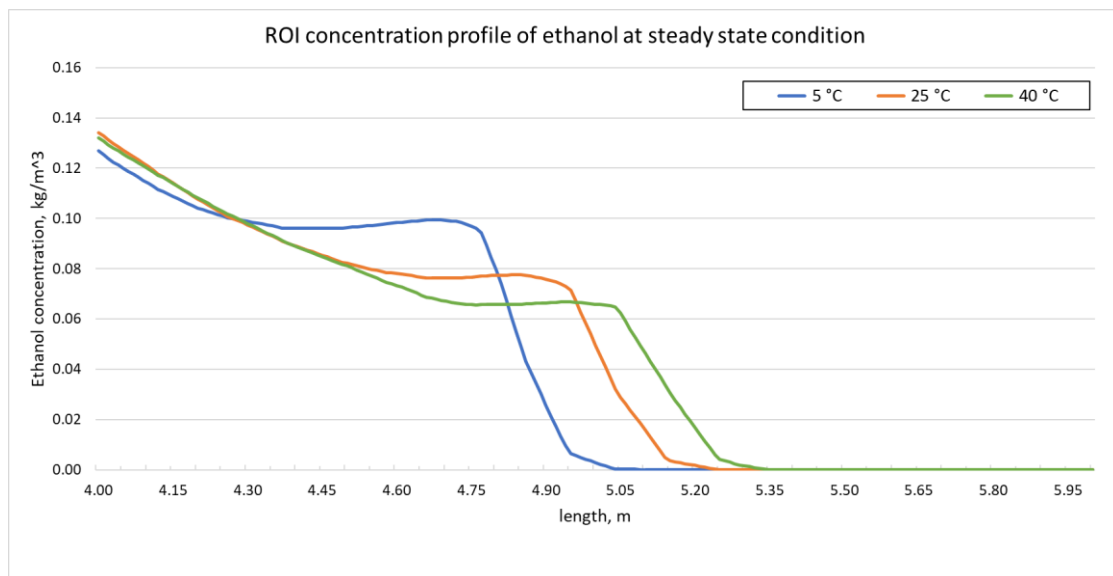


Fig. 11. Ethanol concentration profile at the tip region of the dispersion (steady-state)

Table 4 and 5 shows the maximum distance of the dispersion at different ambient temperature and the percentage change of the length of dispersion by referring to 5°C as the initial distance.

Table 4

The distance of the dispersion and change percentage (transient, t = 10 seconds)

Ambient Temp. Level	Max. length of dispersion, (m)	Change percentage, (%)
5°C	2.40	-
25°C	2.73	+13.75%
40°C	3.18	+32.50%

Table 5

The distance of the dispersion and change percentage (steady-state)

Ambient Temp. Level	Max. length of dispersion, (m)	Change percentage, (%)
5°C	3.86	-
25°C	4.26	+10.36%
40°C	4.44	+15.03%

4. Conclusions

In conclusion, ambient temperature plays a crucial role in determining the dispersion of harmful gases in indoor environments. The results of the theoretical study and CFD simulation indicate that an increase in the ambient temperature leads to an increase in the spread distance of the gas, while a decrease in ambient temperature results in a decrease in the spread distance. These results provide valuable insights into the importance of temperature control in mitigating the spread of harmful gases in indoor environments. By managing temperature effectively, industrial and residential settings can reduce the risk of harmful gas incidents, which pose significant threats to public health and safety. It is imperative to further research this issue to develop more effective methods of temperature control, and to enhance our understanding of the mechanisms behind gas dispersion in indoor environments.

Acknowledgement

The author would like to acknowledge the financial support through the Fundamental Research Grant Scheme (FRGS) under the grant number of FRGS/1/2022/TK08/UNIMAP/02/65 from the Minister of Education Malaysia.

References

- [1] Visvanathan, Retnam, Kamarulzaman Kamarudin, Syed Muhammad Mamduh, Masahiro Toyoura, Ahmad Shakaff Ali Yeon, Ammar Zakaria, Latifah Munirah Kamarudin, Xiaoyang Mao, and Shazmin Aniza Abdul Shukor. "Improved mobile robot-based gas distribution mapping through propagated distance transform for structured indoor environment." *Advanced Robotics* 34, no. 10 (2020): 637-647. <https://doi.org/10.1080/01691864.2020.1748900>
- [2] Kourkouta, Lambriini., Christos Iliadis, Petros Ouzounakis, and Alexandros Monios. "Dangerous gases and poisonings: A literature review." *J Health Commun* 3, no. 2 (2018): 26. <https://doi.org/10.4172/2472-1654.100136>
- [3] Broughton, Edward. "The Bhopal disaster and its aftermath: a review." *Environmental Health* 4, no. 1 (2005): 1-6. <https://doi.org/10.1186/1476-069X-4-6>
- [4] "Visakhapatnam Gas Leak: 200 Women Fall Sick after Inhaling Ammonia." *The Times of India*. June 4, 2022.
- [5] "Natural Gas." American Gas Association, February 13, 2023.
- [6] Niaz, Mansoor. "A Rational Reconstruction of the Kinetic Molecular Theory of Gases Based on History and Philosophy of Science and Its Implications for Chemistry Textbooks." *Instructional Science* 28, no. 1 (2000): 23–50. <https://doi.org/10.1023/A:1003429101358>
- [7] George, Arnold, and Clem Zidick. "Charles's law revisited." *Journal of chemical education* 68, no. 12 (1991): 1042. <https://doi.org/10.1021/ed068p1042>
- [8] Breck, W. G., and F. W. Holmes. "An experimental approach to the ideal gas law." *Journal of Chemical Education* 44, no. 5 (1967): 293. <https://doi.org/10.1021/ed044p293>
- [9] Zarzycki, Roman, and Andrzej Chacuk. "Interphase Mass Transfer." *Absorption*, 1993, 167–204. <https://doi.org/10.1016/B978-0-08-040262-8.50010-1>
- [10] Himmelblau, D. M., and K. B. Bischoff. "Mass Transfer." *Industrial & Engineering Chemistry* 58, no. 12 (1966): 32–41. <https://doi.org/10.1021/ie50684a007>
- [11] Zhuang, William. "Theoretical and numerical studies on transport of gaseous contaminants in ventilated indoor environment." PhD diss., RMIT University, 2015.
- [12] Yang, Dongdong, Guoming Chen, and Ziliang Dai. "Accident modeling of toxic gas-containing flammable gas release and explosion on an offshore platform." *Journal of Loss Prevention in the Process Industries* 65 (2020): 104118. <https://doi.org/10.1016/j.jlp.2020.104118>

- [13] Lim, Hwiyeoung, Kisung Um, and Seungho Jung. "A study on effective mitigation system for accidental toxic gas releases." *Journal of Loss Prevention in the Process Industries* 49 (2017): 636-644. <https://doi.org/10.1016/j.jlp.2017.05.017>
- [14] Min, Dong Seok, Shinhee Choi, Eui-young Oh, Jechan Lee, Chang-Gu Lee, Kwon-young Choi, and Seungho Jung. "Numerical modelling for effect of water curtain in mitigating toxic gas release." *Journal of Loss Prevention in the Process Industries* 63 (2020): 103972. <https://doi.org/10.1016/j.jlp.2019.103972>
- [15] Dasgotra, Ankit, GVV Varun Teja, Ankit Sharma, and Kirti Bhushan Mishra. "CFD modeling of large-scale flammable cloud dispersion using FLACS." *Journal of Loss Prevention in the Process Industries* 56 (2018): 531-536. <https://doi.org/10.1016/j.jlp.2018.01.001>
- [16] Yang, Seeyub, Kyeongwoo Jeon, Dongju Kang, and Chonghun Han. "Accident analysis of the Gumi hydrogen fluoride gas leak using CFD and comparison with post-accidental environmental impacts." *Journal of Loss Prevention in the Process Industries* 48 (2017): 207-215. <https://doi.org/10.1016/j.jlp.2017.05.001>
- [17] Argyropoulos, C. D., A. M. Ashraf, N. C. Markatos, and K. E. Kakosimos. "Mathematical modelling and computer simulation of toxic gas building infiltration." *Process Safety and Environmental Protection* 111 (2017): 687-700. <https://doi.org/10.1016/j.psep.2017.08.038>
- [18] Safakar, Mohsen, S. Syafie, and Robiah Yunus. "CFD analysis chlorine gas dispersion in indoor storage: Temperatures with wind velocities effect studies." In *2014 IEEE International Conference on Industrial Engineering and Engineering Management*, pp. 1219-1222. IEEE, 2014. <https://doi.org/10.1109/IEEM.2014.7058832>
- [19] Ansys, Inc. "ANSYS FLUENT theory guide." *Canonsburg, Pa* 794 (2011).
- [20] Syed Zakaria, Syed Muhammad Mamduh, Retnam Visvanathan, Kamarulzaman Kamarudin, Ahmad Shakaff Ali Yeon, Ali Yeon Md. Shakaff, Ammar Zakaria, and Latifah Munirah Kamarudin. "Development of a scalable testbed for mobile olfaction verification." *Sensors* 15, no. 12 (2015): 30894-30912. <https://doi.org/10.3390/s151229834>
- [21] Kamarudin, Kamarulzaman. "An Improved Mobile Robot Based Gas Source Localization with Temperature and Humidity Compensation via SLAM and Gas Distribution Mapping." PhD diss., School of Mechatronic Engineering, 2016.
- [22] Abdullah, Abdunasser Nabil, Kamarulzaman Kamarudin, Syed Muhammad Mamduh, Abdul Hamid Adom, and Zaffry Hadi Mohd Juffry. "Effect of environmental temperature and humidity on different metal oxide gas sensors at various gas concentration levels." In *IOP Conference Series: Materials Science and Engineering*, vol. 864, no. 1, p. 012152. IOP Publishing, 2020. <https://doi.org/10.1088/1757-899X/864/1/012152>
- [23] Kamarudin, Kamarulzaman, Syed Muhammad Mamduh, Ali Yeon Md Shakaff, Shaharil Mad Saad, Ammar Zakaria, Abu Hassan Abdullah, and Latifah Munirah Kamarudin. "Flexible and autonomous integrated system for characterizing metal oxide gas sensor response in dynamic environment." *Instrumentation Science & Technology* 43, no. 1 (2015): 74-88. <https://doi.org/10.1080/10739149.2014.963865>
- [24] Cussler, Edward Lansing. *Diffusion: mass transfer in fluid systems*. Cambridge university press, 2009. <https://doi.org/10.1017/CBO9780511805134>